

# Study on Enhancing Oil Recovery Factor Mechanism of Complex Fault Block Reservoir by WAG Flooding

Yong Tang<sup>1</sup>, Chen YINUO<sup>1</sup>, Qin Jiazheng<sup>1\*</sup>, He Youwei<sup>1</sup>, Duan Shengcai<sup>2</sup>

1. State Key Laboratory of Reservoir Geology and Exploitation, Southwest Petroleum University, Chengdu 610500, Sichuan, China;

2. Hade production oil and gas management area of Tarim Oilfield

(\*Correspondence should be addressed to [jqin@swpu.edu.cn](mailto:jqin@swpu.edu.cn))

## ABSTRACT

At present, CO<sub>2</sub> is one of the main media for gas injection to enhance oil recovery in low permeability reservoirs with good mining application. The development of complex fault block reservoirs has problems such as strong non-homogeneity, difficult injection, low production, etc. In this paper, we carried out a study on the mechanism of WAG flooding to improve the recovery rate in complex fault block reservoirs. Firstly, using 2D profile experiments, it is clarified that gravity overlap and the expansion of swept volume in WAG flooding are the main mechanisms for production increase. Secondly, phase fitting is carried out by combining the field geological data and production data to provide a fluid model for the subsequent numerical simulation study. Finally, the reservoir development method as well as the injection and recovery parameters are studied separately based on the injection and recovery well network model. The simulation results show that the current gas injection pressure can realize the miscible flooding, and the WAG flooding schedule has strong adaptability. The influence of parameter was analyzed through a single factor sensitivity analysis to obtain the optimal injection and extraction parameters. Among them, the well spacing is the main factor affecting the WAG flooding. The results of this study have an important guiding role for the design of CO<sub>2</sub> flooding in complex fault block reservoirs.

**Keywords:** CCUS, low permeability reservoir, CO<sub>2</sub> flooding, WAG, parameters optimization

## 1. INTRODUCTION

Low permeability oil and gas resources are abundant and potential<sup>[1]</sup>. In 2021, the government prioritizes enhanced oil recovery (EOR) in low-permeability oil and gas reservoirs<sup>[2]</sup>. Low permeability reservoirs usually have characteristics such as high coefficient of variation, high permeability resistance and insufficient natural energy<sup>[3]</sup>. Oil wells generally insufficient energy supply and rapid decline in production in the initial stage of reservoir<sup>[4]</sup>. At present, the development methods of low permeability reservoir mainly include depletion, water flooding and gas flooding. The presence of fractures in complex fault block reservoirs leads to severe water intrusion during water flooding. The gas flooding can be effective in mitigating water flooding<sup>[5]</sup>.

Common gas flooding media include natural gas, CO<sub>2</sub>, N<sub>2</sub> and air in low permeability reservoirs<sup>[6]</sup>. Natural gas flooding is difficult to build gas transportation channel due to the influence of technology and economy. The high oxygen content in the air poses a safety risk. The high economic cost of N<sub>2</sub> has not yet been widely adopted in gas injection. CO<sub>2</sub> is a good oil displacement agent with small viscosity, strong extraction ability and strong injection ability compared with water. CO<sub>2</sub> flooding can effectively reduce crude oil viscosity and improve oil flow ratio. Under certain conditions, CO<sub>2</sub> and crude oil can be miscible, reduce oil-water interfacial tension and improve oil recovery factor. CO<sub>2</sub> flooding is an effective EOR schedule and has achieved good results in mining field<sup>[7]</sup>. At the same time, CO<sub>2</sub> flooding has an impact on the storage of greenhouse gas<sup>[8][9]</sup>.

In the mid-20th century, the Atlantic Refining Company of the United States first found that CO<sub>2</sub> could improve crude oil fluidity<sup>[10]</sup>. In 1952, Whorton was granted the world's first CO<sub>2</sub> flooding patent<sup>[11]</sup>. In 1972, Standard Oil Company of California launched the world's first commercial CO<sub>2</sub> flooding project at SA-CROC in the Kelly-Snyder reservoir<sup>[12]</sup>. In 2001, Canada commissioned what is now the world's largest CCUS-EOR demonstration project: the Weyburn project. Based on statistics, the annual oil production from CO<sub>2</sub> flooding in the US amounted to approximately 16 million tons in 2018. Up to now, there are more than 150 CO<sub>2</sub> flooding projects in the world<sup>[13]</sup>. Since the 21st century, a number of CO<sub>2</sub>-EOR demonstration projects have been set up in China, which has strongly promoted the breakthrough of key technologies of CO<sub>2</sub> flooding and the success of reservoir tests<sup>[14]</sup>. It is found that CO<sub>2</sub> gas channeling will lead to low sweep efficiency in reservoir application, which seriously affects the effectiveness of gas flooding<sup>[15]</sup>.

WAG flooding can effectively inhibit gas breakthrough, delay gas channeling, and improve sweep efficiency compared with CO<sub>2</sub> flooding<sup>[16]</sup>. By integrating the respective characteristics of gas flooding and water flooding, WAG flooding can improve the suction profile, increase seepage resistance, control mobility and stabilize the displacement front<sup>[17]</sup>. And WAG flooding has better adaptability to the WAG injection of various heterogeneous layers<sup>[18]</sup>. Dehghan (2012) studied the main mechanism of oil-water-gas interaction in the matrix/fracture network during WAG flooding<sup>[19]</sup>. Gao (2015) experimentally confirmed that CO<sub>2</sub> injection is conducive to recover the crude oil in smaller pores, while the WAG mainly recover more oil from larger pore throats<sup>[20]</sup>. Perera (2016) examined the effective factors in the CO<sub>2</sub>-EOR process: the CO<sub>2</sub> injection rate, flooding volume and well spacing have almost equally important influence on oil production, and the water injection rate creates the minimum influence on oil production<sup>[21]</sup>. Afzali(2020) adopted the implicit pressure Explicit saturation (IMPES) method to model the three-phase flow of near-miscible WAG process and investigated the effect of different parameters on the WAG performance<sup>[22]</sup>. Zhou Feng (2021) established a 2D reservoir CO<sub>2</sub> flooding seepage model based on the classical 2D convection

diffusion equation, summarized the distribution pattern of CO<sub>2</sub> mass concentration and guided the field gas injection development of the reservoir<sup>[23]</sup>. Chai X (2022) found that the production of WAG flooding in tight reservoirs is mainly influenced by the amount of sand entering the ground the thickness of the reservoir and the amount of liquid entering the ground<sup>[24]</sup>. Zhao Lekun (2023) found that with the increase of heterogeneity in the low-permeability reservoir, the earlier the injection time, the more significant the inhibition effect on gas channeling<sup>[25]</sup>.

After years of technical research and field practice, the theory and technology of CO<sub>2</sub> flooding in low permeability reservoirs have begun to take shape. But CO<sub>2</sub> flooding is rarely applied in complex fault block reservoirs in China. This paper establishes the corresponding numerical model according to the geological characteristics of JN reservoir. Comparison and analysis of the oil flooding effect of different development methods, optimization of WAG flooding injection and recovery parameters. This paper provides technical ideas for CO<sub>2</sub>-WAG flooding in complex fracture block reservoirs. Fig 1 shows the flowchart of this paper.

## 2. WAG FLOODING MECHANISM

### 2.1 Geological characteristics of reservoir

JN reservoir is located in a fault-developed formation with complex structure. The reservoir lithology is dominated by fine sandstone with medium quality, low viscosity and low sulfur content of the crude oil. The specific parameters of the reservoir are shown in Table 1. The JN reservoir exhibits poor physical properties, high bound water saturation, significant heterogeneity, and developed faults. The near-wellbore permeability is improved after fracturing the reservoir, the productivity of the well increases slightly and then decreases rapidly, and the oil recovery factor is still low. During water flooding, issues such as restricted water absorption capacity and susceptibility to both water content and injection rate significantly impact the efficiency of the flooding process. Water injection presents challenges related to energy replenishment difficulties, elevated injection pressures affecting well longevity, and potential alterations in reservoir seepage due to capillary pressure effects. Collectively, these factors present impediments for

achieving enhanced oil recovery rates during later stages of production.

## 2.2 Experiment

According to different displacement types, simulations were conducted to observe and compare the displacement processes and profiles using samples such as formation water, simulated oil and CO<sub>2</sub>. The specific experimental procedures include sand filling, pressure test, vacuum pumping, determination of pore volume and permeability, saturated oil sample, pressure buildup and displacement. The experiment concluded following the injection of 1.2PV fluid. Detailed experimental schedule is presented in Table 2, while the experimental setup is depicted in Fig 2. Under different injection amounts, the post-displacement profile is shown in Fig 3. The relationship between injection amount and oil recovery factor is shown in Fig 4.

The 2D section experiment shows: WAG flooding exhibits the highest oil recovery factor at 35.79%, whereas water flooding yields the lowest at 20.51%. Due to the presence of gravity displacement in the profile model, water flooding breaks through first and the recovery rate is

the lowest. The gas flooding profile does not show a distinct oil-gas interface, suggesting potential mass transfer between CO<sub>2</sub> and oil. Gas flooding results in the formation of a gas cap at the top, displacing crude oil from the upper layers, thereby achieving better oil recovery compared to water flooding. The primary mechanism for enhancing production in WAG flooding involves expanding the divergence of gas and water displacement directions, with gravity overlap and gas channeling representing key factors influencing the effectiveness of WAG flooding.

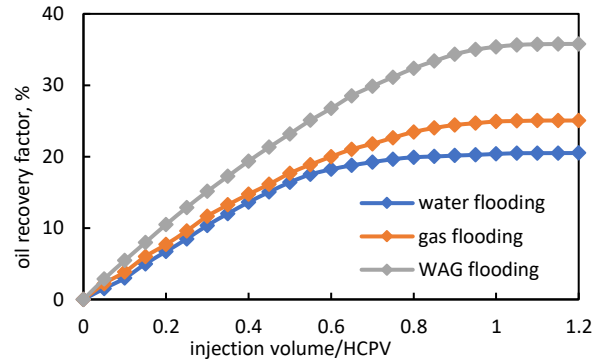


Fig. 4. Comparison of injection amount and oil recovery factor in different displacement modes.

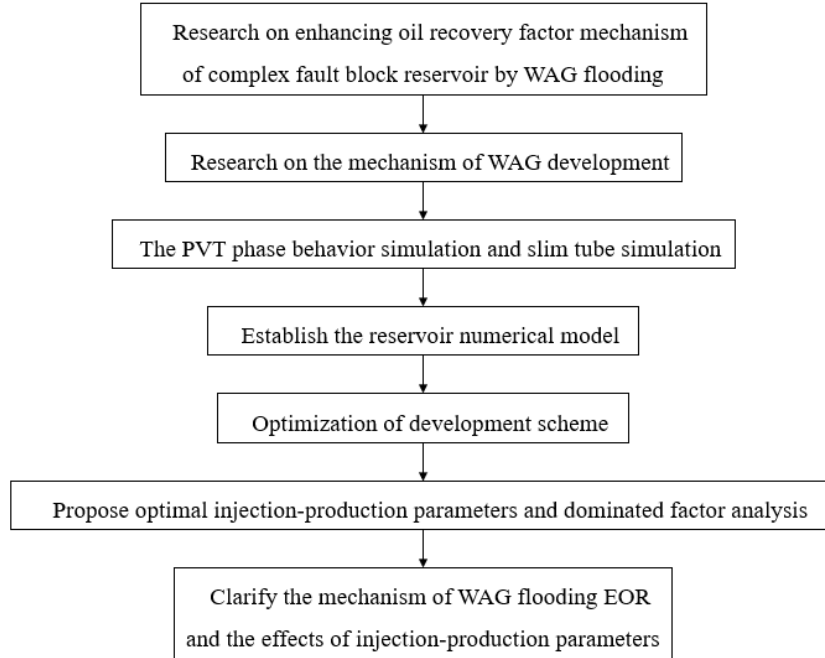


Fig. 1. Flowchart of the work.

Table. 1. Oil reservoir parameter.

Porosity, %	Permeability, $\mu\text{m}^2$	Salinity, g/L	Pressure, MPa	Temperature, $^{\circ}\text{C}$	Pressure factor	Geothermal gradient, $^{\circ}\text{C}/\text{km}$
13.82	$0.84 \times 10^{-3}$	26.72	20.22	79.11	0.91	35

### 3. NUMERICAL SIMULATION

#### 3.1 Fluid model

The fitted formation fluid is extracted from the reservoir fluid, and the composition of the original formation fluid is divided and reorganized into 6 pseudo-components, as shown in Table 3. According to the content of the well flow fluid components, the reservoir fluid is determined to be a typical black oil reservoir.

Table 3. Fluid component partitioning.

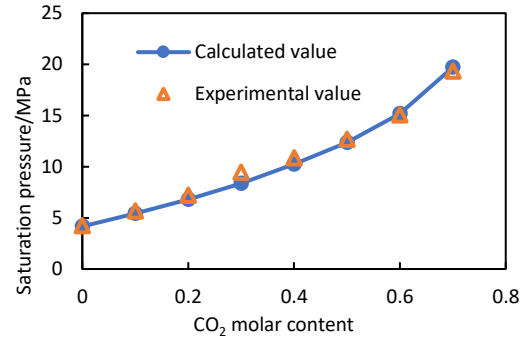
Component	mol%
CO <sub>2</sub>	0.295
C <sub>1</sub>	12.092
C <sub>2</sub> ~C <sub>6</sub>	5.437
C <sub>7</sub> ~C <sub>10</sub>	15.571
C <sub>11</sub> ~C <sub>19</sub>	32.416
C <sub>20</sub> ~C <sub>36</sub>	34.189

The results of the single flash experiment are presented in Table 4. The relative errors after fitting of 1.24%, 0.1%, and 0.25%. The fluid model can meet the needs of subsequent phase simulation calculation and component reservoir simulation.

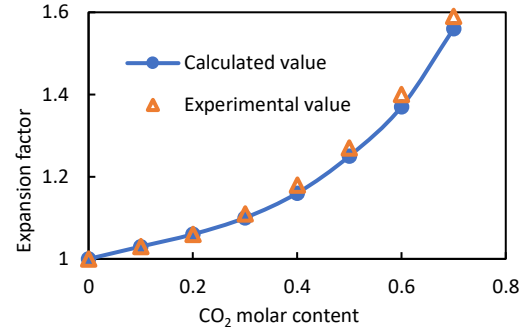
The gas injection expansion fitting can provide the fluid PVT (pressure, volume and temperature) parameter reservoir that accurately reflects the phase transition of the fluid during gas injection. The fitting results are shown in Fig 5. The accuracy of the fitting results is highly accurate and can meet the requirements of subsequent numerical simulation studies.

Table 4. The saturation pressure is compared with the experimental and calculated values of a single flash.

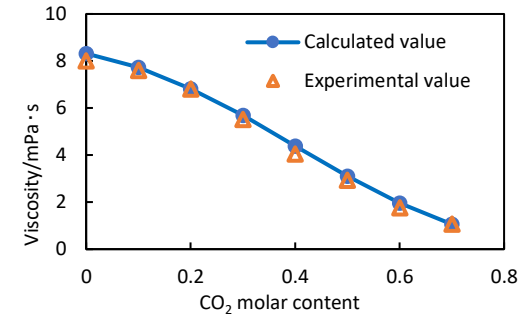
Parameter	Experiment value	Fitted value	Relative error, %
Degassed oil density, g/cm <sup>3</sup>	0.884	0.873	1.24
Single flash gas-oil ratio, m <sup>3</sup> /m <sup>3</sup>	16.49	16.47	0.10
Saturation pressure, MPa	4.184	4.173	0.25



(a)



(b)



(c)

Fig. 5. Expansion experiment and simulation results of CO<sub>2</sub> injection.

The critical parameters of the pseudo-components can be further determined through parameter regression and fitting by adjusting the pseudo-component parameters. The adjusted critical parameters are shown in Table 5.

The detailed parameters of the tube used in this experiment are shown in Table 6. The parameters: the number of grids was 80×1×1, the grid step size was l=0.25m, J=K=0.0044m, and the grid model was shown in Fig 6, Table 7 displays the oil recovery factor by injecting gas under different pressures.

Table 5 Table of critical parameters of pseudo-component of reservoir fluid.

component	molecular weight, g·mol <sup>-1</sup>	Critical pressure, atm	Critical temperature, K	Critical volume, mol <sup>-1</sup>	Acentric factor	Equation coefficient, $\Omega_A$	Equation coefficient, $\Omega_B$
CO <sub>2</sub>	44.01	72.80	304.20	0.094	0.22	0.46	0.07780
CH <sub>4</sub>	16.04	45.40	190.60	0.099	0.01	0.46	0.07780
C <sub>2</sub> ~C <sub>6</sub>	56.36	38.85	399.14	0.241	0.19	0.46	0.07780
C <sub>7</sub> ~C <sub>10</sub>	116.19	27.64	588.58	0.453	0.38	0.46	0.08441
C <sub>11</sub> ~C <sub>19</sub>	203.22	22.51	723.49	0.795	0.66	0.46	0.09336
C <sub>20</sub> ~C <sub>36</sub>	278.44	14.57	672.55	1.252	0.98	0.46	0.07102

Table 6 The slim tube parameters.

Diameter, mm	Length, cm	Pore volume, cm <sup>3</sup>	Porosity, %	Permeability, $\mu\text{m}^2$
4.4	2000	119.91	39.43	10.8

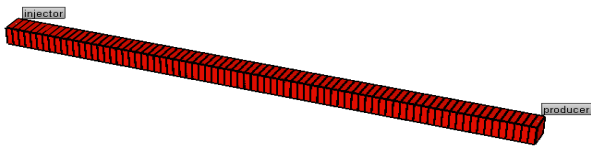


Fig 6 One-dimensional slim tube model.

Table 7 Oil recovery factor by injecting gas under different pressures.

Injection pressure, MPa	Oil recovery factor
18	55.72
21	69.48
24	86.63
27	90.26
30	92.19
33	93.84

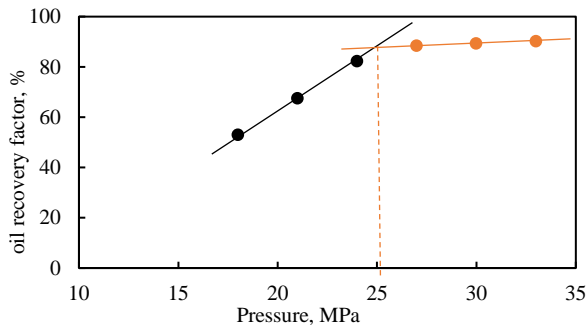


Fig 7 The MMP for the slim-tube simulation.

The result is shown in Fig 7. According to the criteria of miscibility, it can be determined that the MMP under the formation temperature is 24.74MPa. The MMP of slim tube simulation is 25.12MPa and the error is 1.54%. From the current development situation, the permeability of JN

reservoir is low and the difference of driving pressure is obvious. CO<sub>2</sub> flooding EOR can only achieve miscible flooding of reservoir crude oil in part of time and part of the region, and immiscible flooding in other cases.

### 3.2 Numerical model

The 5-spot well pattern is suitable for the blocks with low viscosity and scattered reservoir distribution with high ratio of injection-production wells and multiple effective directions. In this simulation, a 5-spot well pattern system was established, as shown in Fig 8. The grid was divided into 43×43×16 with a well spacing was 300m. The permeability was heterogeneous with an average porosity of 13.82% and an average permeability of  $0.84 \times 10^{-3} \mu\text{m}^2$ . The reservoir driving energy was characterized by elastic energy without edge-bottom water.

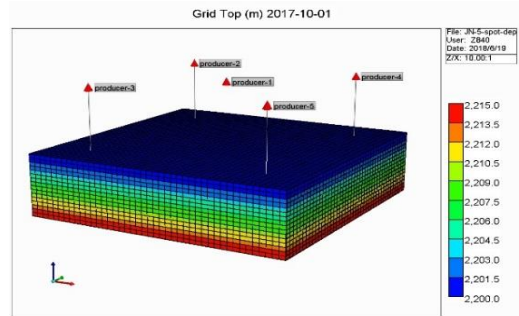


Fig. 8. The 3D grid of the model.

The oil-water and gas-liquid permeability curves are shown in Fig 9 and Fig 10 below. The reservoir is a hydrophilic reservoir with high bound water saturation.

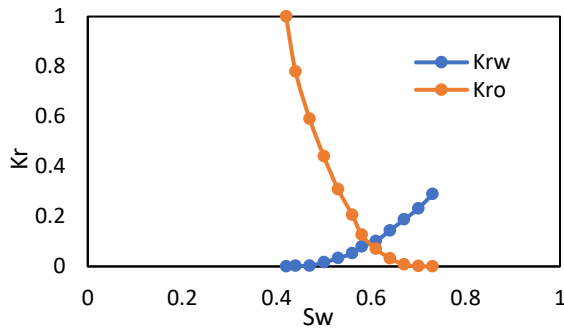


Fig. 9. Oil-water relative permeability curve.

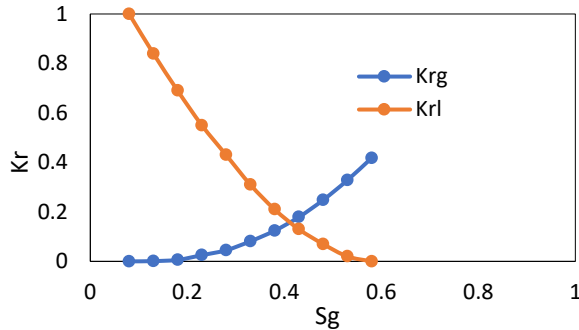


Fig. 10. Gas-liquid relative permeability curve.

#### 4. DEVELOPMENT SCHEME OPTIMIZATION

Based on the reservoir test data and numerical model, four sets of development schedules have been designed for optimization: depletion, water flooding, gas flooding, and WAG flooding. The total amount of CO<sub>2</sub> injected in schedule 3 and schedule 4 is the same.

Table. 8. Schedule design table.

	Schedule setting
Case 1	Depletion, 5 production Wells developed, BHP: 10MPa, simulated production time of 20 years.
Case 2	Water flooding, water injection: 30m <sup>3</sup> /d, BHP: 10MPa, and the water production rate reaches 90%.
Case 3	Gas flooding, gas injection: 6000m <sup>3</sup> /d, BHP :10MPa. The well was shut in after the

Table. 9. Different development methods to produce data.

Development scheme	Cumulative oil, 10 <sup>4</sup> m <sup>3</sup>	Recovery factor, %	Final water cut, %	Final gas-oil ratio, m <sup>3</sup> /m <sup>3</sup>
Depletion	2.27	6.78	7.65	16.08
Water flooding	7.19	21.18	85.98	16.52
Gas flooding	8.93	26.27	6.56	1404.16
WAG flooding	10.58	31.18	68.81	1194.32

	Schedule setting
	gas-oil ratio reached 2000m <sup>3</sup> /m <sup>3</sup> .
Case 4	WAG flooding, the alternating cycle: 3 months, water injection: 30m <sup>3</sup> /d, gas injection: 12000m <sup>3</sup> /d, BHP: 10MPa. The well was shut in after the gas-oil ratio reached 2000m <sup>3</sup> /m <sup>3</sup> .

The simulation results presented in Table 9 and the comparison of outcomes obtained through different development methods are illustrated in Fig 11. The enhanced recovery efficiency of gas flooding is better than that of water flooding, and the recovery efficiency of gas flooding is 5.14% higher than that of water flooding. Under the condition of the same injection volume, the EOR of WAG flooding is 10.02% higher than that of water flooding, and 4.88% higher than that of continuous gas injection.

The simulation results are shown Fig 12-15. Due to gravitational differentiation, water flooding predominantly mobilizes the crude oil at the bottom of the reservoir, while gas flooding mainly uses the crude oil at the top of the reservoir. The WAG flooding utilizes the oil at the top and bottom of the reservoir at the same time, which increases the macroscopic swept volume. Alternate injection of water and gas can improve the oil displacement efficiency and sweep efficiency of the reservoir.

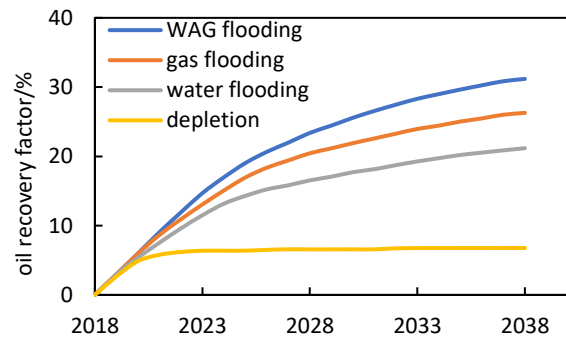


Fig. 11. Oil recovery factor by different development schemes.

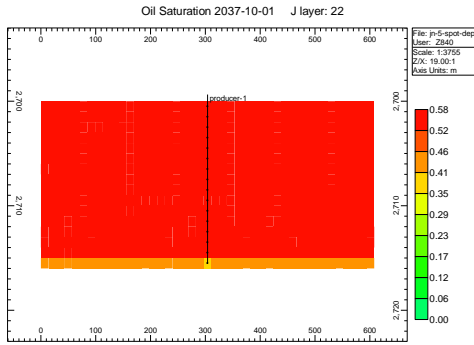


Fig. 12. Depletion.

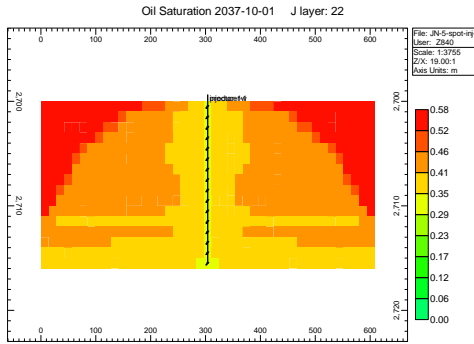


Fig. 13. Water flooding.

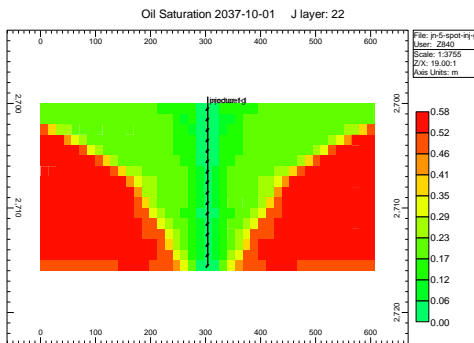


Fig. 14. Gas flooding.

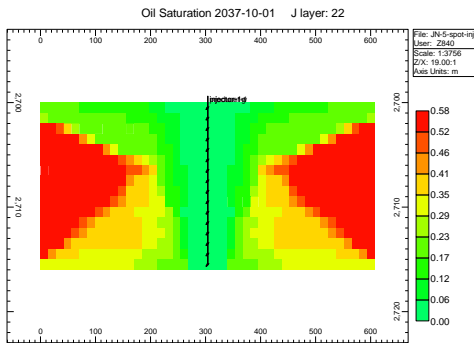


Fig. 15. WAG flooding.

## 5. OPTIMIZATION OF INJECTION-PRODUCTION PARAMETERS

### 5.1 Well spacing

Schedule setting: the daily water injection volume is  $30\text{m}^3/\text{d}$ , the daily  $\text{CO}_2$  injection volume is  $12000\text{m}^3/\text{d}$ , the minimum bottomhole flow pressure is 10MPa, and the well will be shut down when the GOR reaches  $2000\text{m}^3/\text{m}^3$  or the water production rate reaches 90%. The well spacing intervals are 240m, 300m, 360m, and 420m respectively. The comparison of recovery efficiency of different well spacing is shown in Fig 16. With the increase of well spacing, crude oil recovery increases first and then decreases. The time of gas channeling and the utilization rate of  $\text{CO}_2$  are decreased with the well spacing reduction. According to the GOR data, the  $\text{CO}_2$  utilization efficiency and oil recovery efficiency are the highest when the injection-production well spacing is 360m.

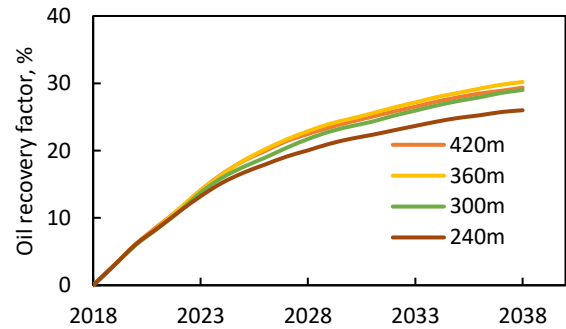


Fig. 16. Oil recovery factor with different well spacing.

### 5.2 Injection time

Schedule setting: when the formation pressure is reduced to 20MPa, 18MPa, 16MPa, 14MPa and 12MPa respectively, constant pressure injection of water and gas is carried out, and the BHP is 10MPa. Simulation results are presented in Table 11, and the comparison of recovery efficiency at different injection times is shown in Fig 17. It is observed that earlier injection times correspond to higher formation pressures and increased oil recovery efficiency. When the injection pressure is maintained at 20MPa, the oil recovery factor can reach up to 32.99%.

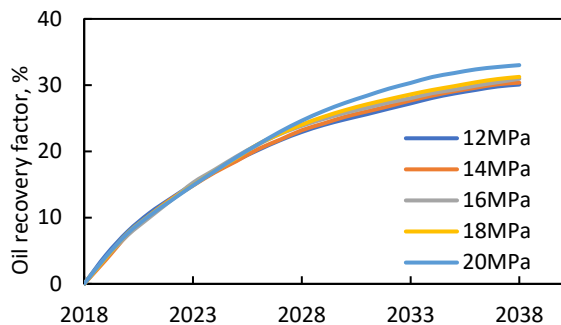


Fig. 17. Oil recovery factor at different injection times.

### 5.3 Injection rate

Schedule setting: the injection speed is set to be 8000m<sup>3</sup>/d, 10000m<sup>3</sup>/d, 12000m<sup>3</sup>/d and 14000m<sup>3</sup>/d, respectively. The simulation results are shown in Fig 18. The simulation results indicate that a higher gas injection rate leads to an increased recovery rate. Excessively fast gas injection results in elevated displacement pressure, leading to preferential flow through large pores and reduced sweep range, consequently causing a rapid increase in the GOR. The optimal injection speed of 12000~14000m<sup>3</sup>/d yields the highest oil production at a final recovery rate of 34.19% and a GOR of 641.77m<sup>3</sup>/m<sup>3</sup>.

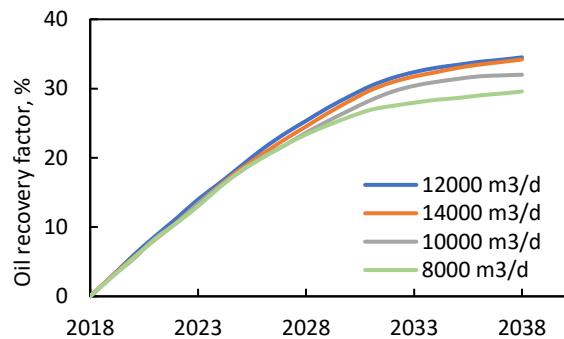


Fig. 18. Oil recovery factor at different injection rates.

### 5.4 Injection volume

Schedule setting: According to the optimal gas injection speed of 14000m<sup>3</sup>/d, the total injection amount is 6×10<sup>4</sup>t, 7×10<sup>4</sup>t, 8×10<sup>4</sup>t, 9×10<sup>4</sup>t and 10×10<sup>4</sup>t respectively. After the total amount of gas injection is reached, continuous water injection is carried out, the daily water injection is 30m<sup>3</sup>/d, and the well is shut down when the GOR reaches 2000m<sup>3</sup>/m<sup>3</sup> or the water production rate reaches 90%. The simulation results are shown in Fig 19. With the increase in CO<sub>2</sub> injection, cumulative oil recovery and recovery initially increase before reaching a peak and

then decrease. Therefore, the optimal injection volume is 6~8×10<sup>4</sup>t.

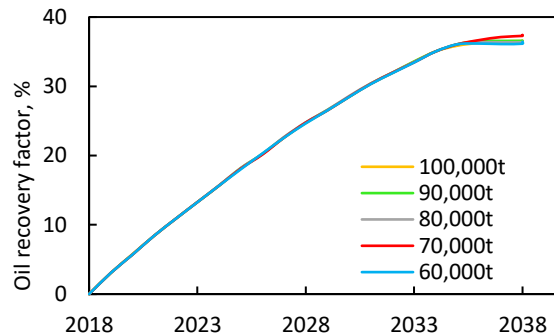


Fig 19 Oil recovery factor at different injection rates.

### 5.5 Oil producing rate

Schedule setting: the daily fluid of different single-well is 5m<sup>3</sup>/d, 6m<sup>3</sup>/d, 7m<sup>3</sup>/d, 8m<sup>3</sup>/d, 9m<sup>3</sup>/d, 10m<sup>3</sup>/d. The simulation results are shown in Fig 20. With the increase of the fixed production fluid, the crude oil recovery factor increases first and then decreases. Regulating the fluid production rate is crucial for controlling reservoir pressure. The CO<sub>2</sub> displacement efficiency is higher when the formation pressure is higher during the development, but the development effect of the oil reservoir with small daily fluid is slow. Consequently, the optimal oil production speed is 6m<sup>3</sup>/d.

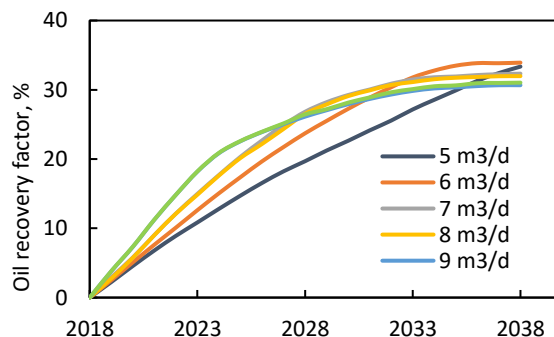


Fig 20 Oil recovery factor at different oil production rates.

### 5.6 Alternating cycle

Schedule setting: injection pressure 20MPa, production well minimum BHP 10MPa. Under the same conditions of other injection parameters, the alternating cycles of water and gas were 3 months, 6 months, 9 months and 12 months, respectively. The simulation results are shown in Fig 21. Based on the simulation results, a shorter cycle leads to higher recovery efficiency. The gas-water mixing transition zone between the segment plugs

formed by gas injection and water injection increases with the alternation cycle is shortened. The mixing transition zone can more effectively slow down the micro-pointing and macro coning of CO<sub>2</sub>, and improve the efficiency of CO<sub>2</sub> drive wave. When the injection cycle is 3 months, the maximum oil recovery factor is 36.74%, indicating that a preferred alternate cycle of 3 months is recommended.

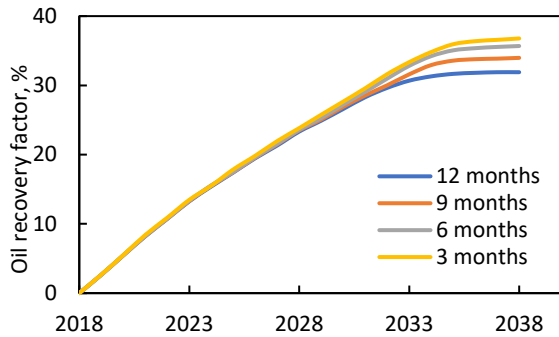


Fig 21 Oil recovery factor with different alternate cycles.

### 5.7 Parameters sensitivity analysis

The study compares the impact of varying factors such as well spacing, injection time, and injection rate on oil recovery. It analyzes the range of each factor's influence on improving oil recovery and compares their sensitivities. Based on the analysis and calculations, the following is observed regarding each factor's influence on recovery efficiency: well spacing, oil production rate, injection volume, injection timing, alternate cycle, and injection rate.

Table 10 Single factor evaluation index range analysis results.

Parameter	Recovery factor		
	Evaluation index	Range	Sensitivity ranking
Well spacing	0.18~0.46	0.26	1
Injection time	0.04~0.14	0.1	4
Injection rate	0.19~0.23	0.04	6
Injection volume	0.01~0.16	0.15	3
Daily oil producing rate	-0.08~0.09	0.17	2
Alternate cycle	0.20~0.26	0.06	5

## 6. CONCLUSIONS

Based on the results presented in this study, the following conclusion can be drawn.

(1) The geological conditions of the target block are complicated, and water flooding has problems such as

difficult injection and water channeling. The WAG flooding can not only expand the affected area, but also effectively alleviate gas channeling and timely supplement formation energy, and the final recovery rate is increased by 4.88%.

(2) The 2D section experiment shows that the recovery rate of WAG flooding is the best (35.79%); the mechanism of enhancing oil recovery by WAG is to expand the swept volume by cooperating with different displacement directions of gas and water, and gravity overlap and gas channeling are the main factors affecting the effect of WAG flooding.

(3) The optimal injection and production parameters include the well spacing (360m), daily oil production rate (per well: 6m<sup>3</sup>/d), alternating cycle (3months), injection rate (12000~14000m<sup>3</sup>/d), and total injection volume (6~8×10<sup>4</sup>t) can yield good EOR performance.

(4) According to the results of sensitivity analysis, well spacing exhibits the highest sensitivity when recovery efficiency is considered as an evaluation criterion. Therefore, in reservoir tests, enhancing sweep efficiency should be prioritized by optimizing well spacing.

### DECLARATION OF INTEREST STATEMENT

The authors declare that they have no known competing financial interests or personal relationships that could have appeared to influence the work reported in this paper. All authors read and approved the final manuscript.

### REFERENCE

- [1] Wenrui, et al. Development of the theory and technology for low permeability reservoirs in China. *Petroleum Exploration and Development* 2018;45.4: 685-697.
- [2] Li Y, Zhao Q, Xue Z. Carbon dioxide capture, utilization and storage technology and industrialization development path under the "double carbon" goal. *Oil Drilling & Production Technology* 2023;45.06: 655-660.
- [3] Qi C, Li R, Zhu S, et al. Pilot test on CO<sub>2</sub> flooding of Chang 4+5<sup>1</sup>oil reservoir in Yougou region of the Ordos Basin. *Oil Drilling & Production Technology* 2019;41.02: 249-253.
- [4] Liu H, Cao G. Opportunities and challenges for scientific and technological innovation and development of oil and gas production engineering in the new era. *Oil Drilling & Production Technology* 2022;44.5: 529-539.
- [5] YUAN S, et al. Progress and prospect of gas injection

- technology for enhanced oil recovery. *Acta Petrolei Sinica* 2020;41.12: 1623-1632.
- [6] HE H, HU X, ZHUANG Y, et al. Study and application of CO<sub>2</sub> flooding parameters optimization in low permeability reservoir: A case study of Block A in Shengli Oilfield. *Petroleum Geology and Recovery Efficiency* 2023;30.02:112-121.
- [7] Yongle H U, et al. Technologies and practice of CO<sub>2</sub> flooding and sequestration in China. *Petroleum Exploration and Development* 2019;46.4: 753-766.
- [8] CAO X, LV G, WANG J, et al. Current situation and future research direction of CO<sub>2</sub> flooding technology in Shengli Oilfield. *Reservoir Evaluation and Development* 2020;10.03: 51-59.
- [9] LI S, TANG Y, HOU C. Present situation and development trend of CO<sub>2</sub> injection enhanced oil recovery technology. *Reservoir Evaluation and Development* 2019;9.3 (): 1-8.
- [10] Qin, J., H. Han, and X. Liu. Application and enlightenment of CO<sub>2</sub> flooding technology in the United States. *Pet. Explor. Dev* 2015;42: 209-216.
- [11] Whorton, Leonidas P., Eugene R. Brownscombe, and Alvin B. Dyes. Method for producing oil by means of carbon dioxide. U.S. Patent No. 2,623,596. 30 Dec. 1952.
- [12] Vikara, Derek, et al. CO<sub>2</sub> Leakage During EOR Operations—Analog Studies to Geologic Storage of CO<sub>2</sub>. No. DOE/NETL-2017/1865. National Energy Technology Laboratory (NETL), Pittsburgh, PA, Morgantown, WV, and Albany, OR (United States), 2019.
- [13] Kumar, Narendra, et al. Fundamental aspects, mechanisms and emerging possibilities of CO<sub>2</sub> miscible flooding in enhanced oil recovery: A review. *Fuel* 2022;330: 125633.
- [14] YUAN Shiyi, et al. Progress and prospect of industrialization of carbon dioxide capture, oil displacement and storage. *Petroleum Exploration and Development* 2022;49.04: 828-834.
- [15] Zhang, Lijun, et al. Inspirations from Field-Reservoir CO<sub>2</sub> Flooding with Different Miscible Degrees under Cross-Scale Oil Reservoir Conditions. *ACS omega* 2024;9.13: 14692-14703.
- [16] Wei, Bing, et al. Interactions and phase behaviors between oleic phase and CO<sub>2</sub> from swelling to miscibility in CO<sub>2</sub>-based enhanced oil recovery (EOR) process: a comprehensive visualization study. *Journal of Molecular Liquids* 2017;232: 277-284.
- [17] Rahimi, Vahid, Mohammad Bidarigh, and Peyman Bahrami. Experimental study and performance investigation of miscible water-alternating-CO<sub>2</sub> flooding for enhancing oil recovery in the Sarvak formation. *Oil & Gas Sciences and Technology—Revue d'IFP Energies Nouvelles* 2017;72.6: 35.
- [18] Wang, Yefei, et al. Remaining oil distribution in models with different heterogeneities after CO<sub>2</sub> WAG injection: Visual research by nuclear magnetic resonance technique. *Journal of Central South University* 2021;28.5: 1412-1421.
- [19] Dehghan, A. A., S. Ghorbanizadeh, and Sh Ayatollahi. Investigating the fracture network effects on sweep efficiency during WAG injection process. *Transport in porous media* 2012;93: 577-595.
- [20] Gao, Hui, et al. Impact of secondary and tertiary floods on microscopic residual oil distribution in medium-to-high permeability cores with NMR technique. *Energy & Fuels* 2015;29.8: 4721-4729.
- [21] Perera, Mandadige Samintha Anne, et al. A review of CO<sub>2</sub>-enhanced oil recovery with a simulated sensitivity analysis. *Energies* 2016;9.7: 481.
- [22] Afzali, Shokufe, et al. Mathematical modeling and simulation of water-alternating-gas (WAG) process by incorporating capillary pressure and hysteresis effects. *Fuel* 2020;263: 116362.
- [23] Zhou Feng, Gao Wei, and Xiaoming Li. Mass concentration distribution of CO<sub>2</sub> miscible flooding in two-dimensional porous media. *Fault-Block Oil and Gas Field* 2021;28.1: 120-123.
- [24] Chai X, Tian L, et al. Production Characteristics, Evaluation, and Prediction of CO<sub>2</sub> Water-Alternating-Gas Flooding in Tight Oil Reservoir. *Journal of Energy Resources Technology* 2022;144.3: 033006.
- [25] Zhao, Lekun, et al. Research on the Timing of WAG Intervention in Low Permeability Reservoir CO<sub>2</sub> Flooding Process to Improve CO<sub>2</sub> Performance and Enhance Recovery. *Energies* 2023;16.21: 7373.